Practical Monte Carlo using MCNP
Assessed exercises

Angus Hollands

April 27, 2018

Abstract

A Monte Carlo simulation was performed for 20 000 source histories, to model the light water moderated neutron fluence from a fission neutron source through the sides of a stainless steel bucket. The resulting fluence histograms were recorded, plotted against energy, and the statistical reliability of the data evaluated. One set of tally results were not found to be reliable after failing the tally fluctuation chart (TFC) Figure of Merit (FoM) slope and distribution tests. The simulation was subsequently repeated for a larger number of source histories, and the corresponding statistical reliability of the data re–evaluated. It was found that simulating 210 000 source histories was sufficient for both flux tallies to pass the ten TFC tests, indicating result reliability. A second Monte Carlo model was designed to investigate the effective multiplication factor k_{eff} of a simplified four cylinder enriched uranium reactor system. Several simulations were performed for two moderators (graphite, light water) and two enrichments (20 %^{235}U, 25 %^{235}U). The values for k_{eff} were found (in product order) to be 0.793 40(75), 0.934 39(75), 0.845 32(76), and 1.005 07(78), respectively.

1 Introduction

The Boltzmann neutron transport equation (see Eq 1, for the integral form describing a non multiplying medium with a time–independent source) is a description of the macroscopic processes governing the conservation of neutrons within a system.

$$(\mathbf{\Omega} \cdot \nabla + \Sigma_t(\mathbf{r}, E))\, \phi(\mathbf{r}, E, \mathbf{\Omega}) = \int_{4\pi} \int_0^\infty \Sigma_s(\mathbf{r}, E' \to E, \mathbf{\Omega}' \to \mathbf{\Omega}) \phi(\mathbf{r}, E', \mathbf{\Omega}')\, \mathrm{d}E'\, \mathrm{d}\mathbf{\Omega}' + s(\mathbf{r}, E, \mathbf{\Omega}) \tag{1}$$

Though simple to derive from conventional transport theory, analytical solutions are difficult for simple systems, and effectively impossible for those which are complex. Instead, one must solve the transport equation numerically, either by deterministic or stochastic methods. In the former case, one can discretise the problem along each of its dimensions, and solve a set of matrix equations which describe the behaviour of the (local) system. Though quick to find an approximate solution, its performance is heavily dependent upon the simplicity of the problem, with complex geometries and complicated neutron spectra demanding an explicit compromise between model accuracy and performance. Stochastic methods (or Monte Carlo methods) instead simulate the relevant physical processes themselves, where the parameters of the processes are sampled from known probability distributions. As more and more of the problem space is sampled, the MC solution approaches the "true" solution (distribution). Though computationally expensive, by means of convergence, these methods may be more accurate than the deterministic approach.

As well as the fission–free transport equation, the Monte Carlo approach can also be used to solve the k–eigenvalue transport equation of the form

$$(\mathbf{\Omega} \cdot \nabla + \Sigma_t(\mathbf{r}, E))\, \phi(\mathbf{r}, E, \mathbf{\Omega}) = \int_{4\pi} \int_0^\infty \Sigma_s(\mathbf{r}, E' \to E, \mathbf{\Omega}' \to \mathbf{\Omega}) \phi(\mathbf{r}, E', \mathbf{\Omega}')\, \mathrm{d}E'\, \mathrm{d}\mathbf{\Omega}' + \frac{1}{k} \frac{\chi(E)}{4\pi} s(\mathbf{r}, E, \mathbf{\Omega}) \tag{2}$$

for k, where $\chi(E)$ describes the emission spectrum of the fission neutrons. The largest eigenvalue k quantifies the effective level of neutron multiplication k_{eff} within the system. The state of the system is then given by Table 1

In this report, the Monte Carlo N-Particle (MCNP) code is used to determine the neutron flux along the external walls of a model reactor vessel. The model geometry is defined using the various non–macrobody primitives

Table 1: Criticality inequalities in k

Condition	State
$k < 1$	Sub-critical
$k = 1$	Critical
$k > 1$	Super-critical

available, and the surface tallying feature used to obtain two energy dependent histograms describing the neutron fluence distribution incident upon the problem surfaces. An investigation is performed into the conditions under which these tally data are invalidated. To provide a neutron source for this model, the Watt Fission prompt neutron spectrum for ^{235}U is used, with parameters referenced from the MCNP user manual.
Subsequently, the MCNP KCODE k–eigenvalue transport equation solver is used to investigate the effect of varying parameters such as the moderator material and fuel enrichment upon the reactor criticality.

2 Method

2.1 Exercise 1

An MCNP input file was written to design the simulation model. A stainless steel vessel (of density $7.92\,\mathrm{g/cm^3}$) with internal base 10 cm by 20 cm, wall thickness 2 mm, and external height 20 cm was modelled as the intersection between two cuboids, centered about the z axis with the lower floor placed at $z = 0$. The moderator was defined as

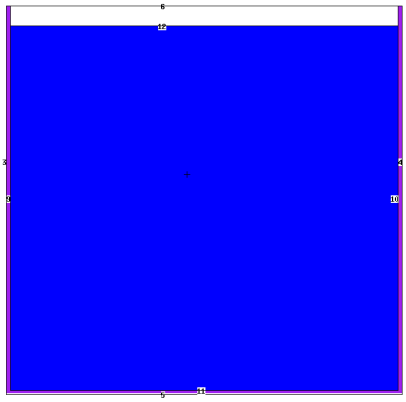

Figure 1: 2D XZ plot of Exercise 1 geometry.

the intersection between the internal cuboid and an infinite planar surface of normal $\begin{pmatrix}0 & 0 & -1\end{pmatrix}$ at $\begin{pmatrix}0 & 0 & 19.0\end{pmatrix}$. Two void regions were then defined, one for the volume outside of the outer cuboid, and the other for the region between the moderator surface and the plane bounding the outer cuboid ceiling.
All cells were defined with a neutron importance of 1, apart from the outer void region, assigned with the correct weight density (apart from the outer void region), and their materials appropriately defined in the DATA section with the appropriate atomic / weight composition. The moderator material was assigned the light water low energy cross section library *lwtr.01[t]*.
Two surface neutron flux tally cards were defined, using a common set of energy bins, with upper bin edges defined along the log–linear interval between 10^{-9} MeV and 10 MeV. One tally recorded the *average* flux through the two short external sides of the vessel, and the other recorded the corresponding flux through the two larger sides.
A thermal neutron source with an energy distribution given by the Watt Fission spectrum for ^{235}U (see Fig 2), with parameters $a = 0.988$, $b = 2.249$, was placed at $\begin{pmatrix}0 & 0 & 2.2\end{pmatrix}$, and the simulation performed for 20 000 neutrons (MODE N) source histories. A secondary simulation was performed with an increased number of source histories of 210 000.

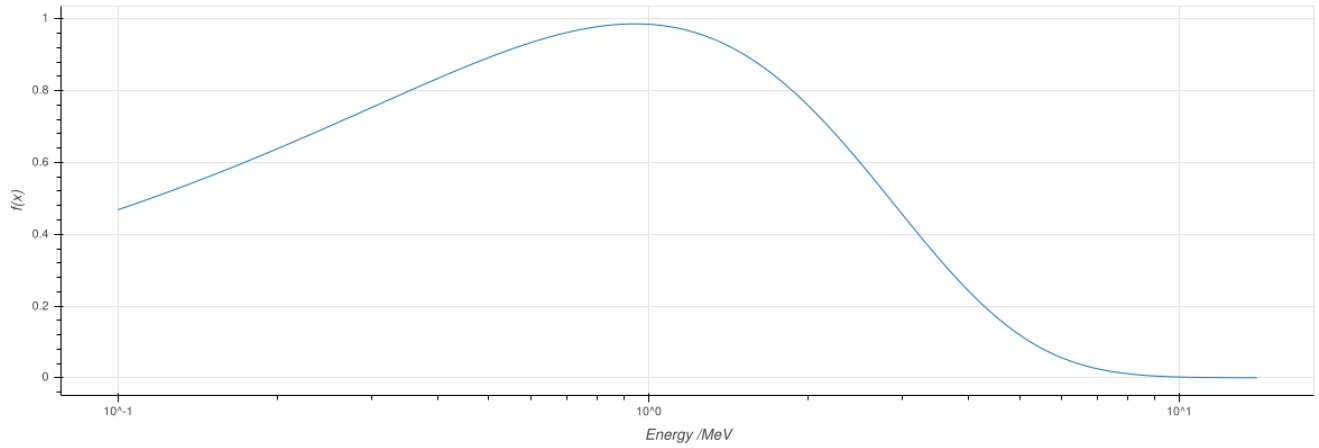

Figure 2: Watt Fission spectrum for prompt neutrons (^{235}U).

2.2 Exercise 3

The geometry described in Section 2.1 was modified such that the internal base measured 100 cm by 100 cm, with an external height of 60 cm. A concrete floor was defined, of thickness 150 cm, and a lateral radius of 200 cm. These two parameters were not defined in the exercise requirements. The former was informed by the thickness of a conventional reactor containment vessel[2] and an approximate 0.025 % attenuation calculation (see Eq 3). From literature, the value of Σ_R is approximately 0.04[1]. The latter was chosen as the radius of the smallest conventional reactor core diameter.

$$I(x) = I_0 \exp(-\mu x) \tag{3}$$

$$\mu = \frac{1}{\Sigma_R} \tag{4}$$

$$x = -\frac{\ln \frac{I(x)}{I_0}}{\mu} \tag{5}$$

The definition of a concrete floor serves an additional purpose to shielding; to reflect a fraction of the neutrons back into the vessel. The moderator volume was resized to satisfy the original wall thickness constraints, and the surface moved to 2 cm from the ceiling of the vessel. For each simulation, the appropriate moderator material was defined (for graphite / water), and the corresponding low energy cross section library referenced (*lwtr.01[t]* / *grph.01[t]*)

Four enriched uranium cylindrical sources, of radius 7.5 cm and height 25 cm, were placed within the moderator cell, which served as fissile material for the KCODE algorithm. Their corresponding material card was defined for a by–weight enrichment which was varied across several of the simulations. The primary neutron sites for the solver were provided as initialisation parameters for the algorithm, using the KSRC card, which distributed 1000 starting neutrons across the centroids of the uranium cylinders. The KCODE algorithm was configured for a warm up of 200 cycles, with an initial reactivity estimate of 1.0 (critical), and run for 1000 active cycles.

In order to permit neutrons to scatter back into the vessel from the concrete floor, the air–gap void cell from the previous model was modified to include the cylindrical volume above the concrete floor, bounded by the plane which defined the upper limit of the vessel walls. This void region was maintained with a neutron importance of 1. A 'graveyard' void region was defined as the volume outside of the concrete floor and primary void cell, assigned a neutron importance of 0.

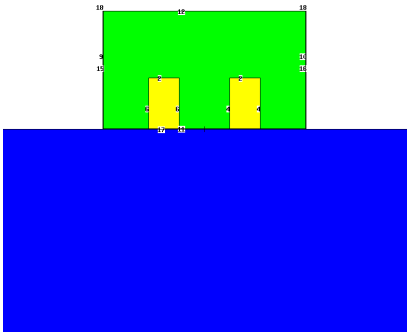

Figure 3: 2D XZ plot of Exercise 3.d. (Graphite) geometry.

3 Results

3.1 Exercise 1

3.1.1 Initial Simulation

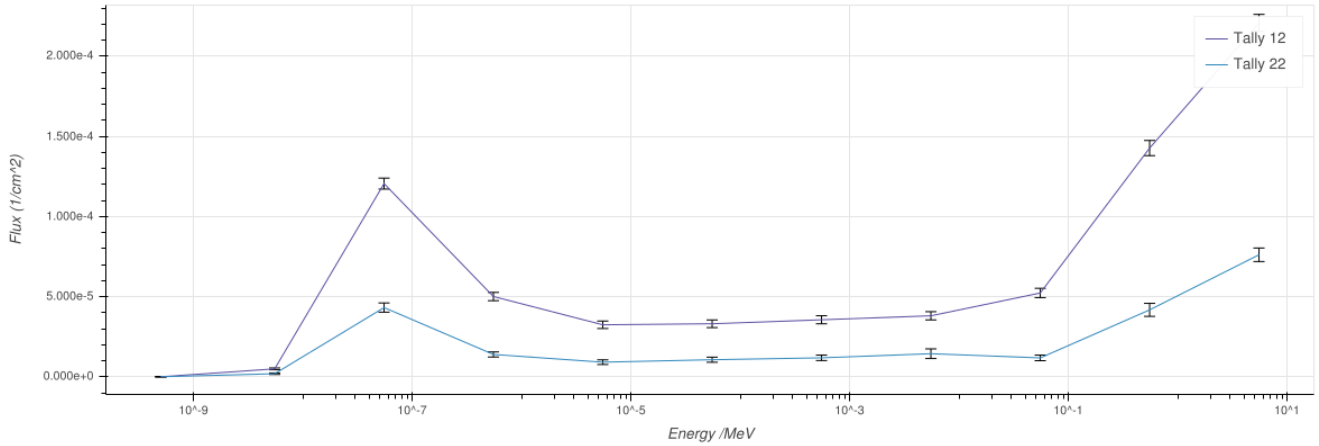

Figure 4: Fluence tallies for external surfaces of container, for 20 000 histories. Tally 12 corresponds to the fluence across the shorter sides of the container, 22 the longer sides.

The tallies are defined as follows:

- Tally 12: The short sides of characteristic length 10 cm
- Tally 22: The long sides of characteristic length 20 cm

For the tallies, MCNP reported that the tallies passed most of the 10 statistical tests for the tally fluctuation chart, which are defined as

1. Mean is randomly distributed
2. Relative error ideally less than 0.10
3. Relative error decreases over time
4. Decrease rate of relative error follows $\frac{1}{\sqrt{\text{nps}}}$
5. Variance of variance ideally less than 0.10

6. Variance of variance decreases over time
7. Decrease rate of variance of variance follows $\frac{1}{\sqrt{\text{nps}}}$
8. Figure of Merit (FoM) is roughly constant
9. FoM is randomly distributed
10. Slope of the FoM pdf is greater than 3.0

The first tally passed all ten tests, whilst Tally 22 failed the FoM slope PDF test (2.46) and FoM distribution test (*increase*). In addition, all tallies had at least one bin with large relative error (> 0.1).
The total fluences across each pair of surfaces were as follows (see Table 2):

- Long sides (Tally 12): $7.300\,35(1220) \times 10^{-4}\,\text{n/cm}^2$
- Short sides (Tally 22): $2.343\,46(3380) \times 10^{-4}\,\text{n/cm}^2$

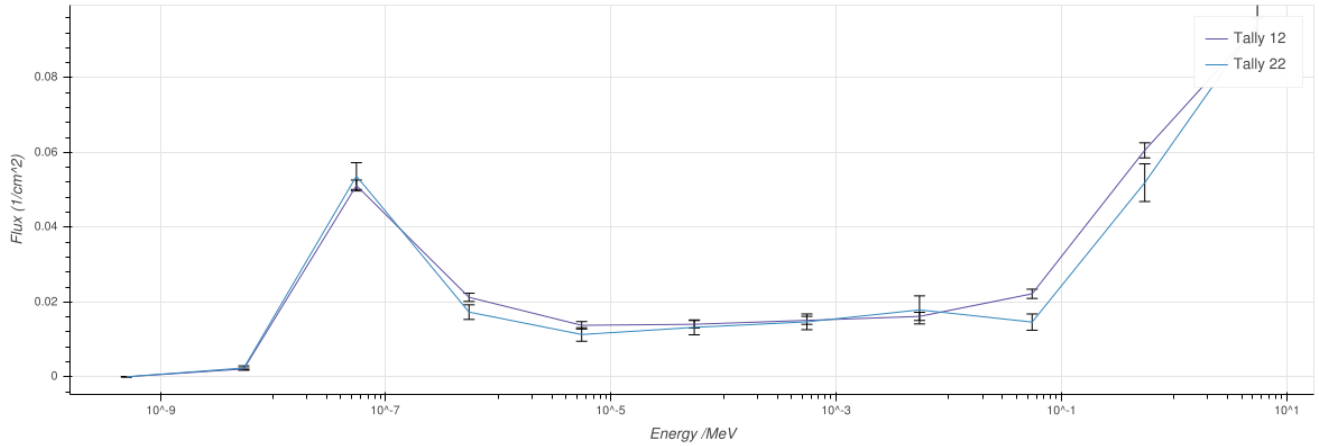

Figure 5: Area normalised fluence tallies for external surfaces of container, for 20 000 histories. Tally 12 corresponds to the fluence across the shorter sides of the container, 22 the longer sides.

3.1.2 Flux

For a source of 10^{10} neutrons per second, the corresponding fluxes would be $7.300\,35(1220) \times 10^{6}\,\text{n/cm}^2/\text{s}$ and $2.343\,46(3380) \times 10^{6}\,\text{n/cm}^2/\text{s}$ respectively.

3.1.3 Increasing Number of Histories

By increasing the particle histories limit to 210 000, the standard uncertainty upon the tally amplitudes diminishes, approximately $\frac{1}{2}$ as expected. The bin amplitude for Tally 22 corresponding to $(10^{-8} < E < 10^{-9})$ did not lie within the uncertainty permitted by its previous value. However, this tally did not pass all statistical tests for 20000 to allow such a constraint in the first place, and so was to be expected. By increasing the number of particle histories to the new limit, all statistical tests were subsequently passed. Furthermore, the difference in neutron energy distribution between the two tallies became more apparent; in particular, in the higher energy regime the two distributions diverged most significantly, with the narrower surfaces (further from the source) showing greater attenuation at higher energies. The recorded fluences were as follows (see Table 2):

- Long sides (Tally 12): $7.343\,20(390) \times 10^{-4}\,\text{n/cm}^2$
- Short sides (Tally 22): $2.298\,16(1030) \times 10^{-4}\,\text{n/cm}^2$

3.2 Exercise 3

Table 2: Fluences of both tallies, for 20 000 and 210 000 histories. Tally 12 corresponds to the fluence across the shorter sides of the container, 22 the longer sides.

	20 000 histories		210 000 histories	
Energy	Fluence(21)	Fluence(22)	Fluence(21)	Fluence(22)
$-\infty < E < 10^{-9}$	0.000 00(0)	0.000 00(0)	$2.887\,92(46130) \times 10^{-8}$	$2.502\,56(72820) \times 10^{-8}$
$10^{-9} < E < 10^{-8}$	$4.911\,46(11510) \times 10^{-6}$	$1.884\,57(24420) \times 10^{-6}$	$4.640\,30(4200) \times 10^{-6}$	$1.728\,82(8570) \times 10^{-6}$
$10^{-8} < E < 10^{-7}$	$1.204\,74(2850) \times 10^{-4}$	$4.314\,31(6680) \times 10^{-5}$	$1.208\,41(910) \times 10^{-4}$	$4.607\,10(2090) \times 10^{-5}$
$10^{-7} < E < 10^{-6}$	$5.002\,77(5160) \times 10^{-5}$	$1.389\,64(11300) \times 10^{-5}$	$4.957\,97(1640) \times 10^{-5}$	$1.653\,72(3870) \times 10^{-5}$
$10^{-6} < E < 10^{-5}$	$3.240\,83(7210) \times 10^{-5}$	$9.081\,58(16070) \times 10^{-6}$	$3.196\,29(2340) \times 10^{-5}$	$9.098\,85(5170) \times 10^{-6}$
$10^{-5} < E < 10^{-4}$	$3.305\,01(7210) \times 10^{-5}$	$1.061\,69(15030) \times 10^{-5}$	$3.258\,05(2370) \times 10^{-5}$	$9.833\,37(6340) \times 10^{-6}$
$10^{-4} < E < 10^{-3}$	$3.553\,19(7070) \times 10^{-5}$	$1.180\,50(14330) \times 10^{-5}$	$3.673\,38(2180) \times 10^{-5}$	$9.159\,55(5580) \times 10^{-6}$
$10^{-3} < E < 10^{-2}$	$3.802\,14(6740) \times 10^{-5}$	$1.437\,14(21010) \times 10^{-5}$	$3.942\,21(2140) \times 10^{-5}$	$1.131\,12(6630) \times 10^{-5}$
$10^{-2} < E < 10^{-1}$	$5.225\,32(5570) \times 10^{-5}$	$1.175\,01(14860) \times 10^{-5}$	$5.282\,30(1800) \times 10^{-5}$	$1.447\,56(4960) \times 10^{-5}$
$10^{-1} < E < 1$	$1.426\,35(3320) \times 10^{-4}$	$4.171\,69(9710) \times 10^{-5}$	$1.466\,73(1040) \times 10^{-4}$	$4.098\,81(2560) \times 10^{-5}$
$1 < E < 10^{1}$	$2.207\,22(2400) \times 10^{-4}$	$7.607\,96(5540) \times 10^{-5}$	$2.190\,35(730) \times 10^{-4}$	$7.058\,70(1680) \times 10^{-5}$

Table 3: k_{eff} for various simulated scenarios.

Moderator	Enrichment	k_{eff}
Light water	20 %	0.793 40(75)
Graphite	20 %	0.934 39(75)
Light water	25 %	0.845 32(76)
Graphite	25 %	1.005 07(78)

4 Analysis

4.1 Exercise 1

The final FoM slope test evaluates whether the central limit theorem has been satisfied; that is, both the first and second moments of the PDF exist (and are therefore finite). The second moment $\int_{\infty}^{\infty} x^2 f(x)\,\mathrm{dx}$ is observed to exist when $f(x)$ decreases faster than $\frac{1}{x^3}$, and hence the final test evaluates this condition. Consequently, in failing this test for the initial simulation, it cannot be concluded that Tally 22 is reliable.

The significant difference between the total fluences for the two tallies can be explained by both the variation in solid angle between the two surfaces (each surface is sufficiently large relative to the distance to the source, that the incident flux varies along the surface), and the difference in neutron absorption along the axes of the detector. The neutron absorption probability through a medium is given by the Beer Lambert law, and is exponential in the distance travelled. The normalised (by area) neutron energy distributions are approximately equal, and what variation there exists between the two tallies lies predominantly within the uncertainty on the recorded values. However, there are several points, particularly in the higher energy regime whose standard errors do not account for the observed deviation. In these cases, the nonlinear attenuation function, which depends upon neutron energy, leads to a distortion of the tallied energy spectrum.

4.2 Exercise 3

4.2.1 Graphite Moderator

When replacing the moderator material with graphite, the effective criticality of the system was observed to increase. The criticality of a reactor depends upon the number of neutrons which are thermalised (by the moderator) and lead to thermal fission in the fuel. In transitioning the moderator material from light water to graphite, the mean logarithmic energy decrement of the moderator ξ decreases (lesser energy loss per collision), such that the

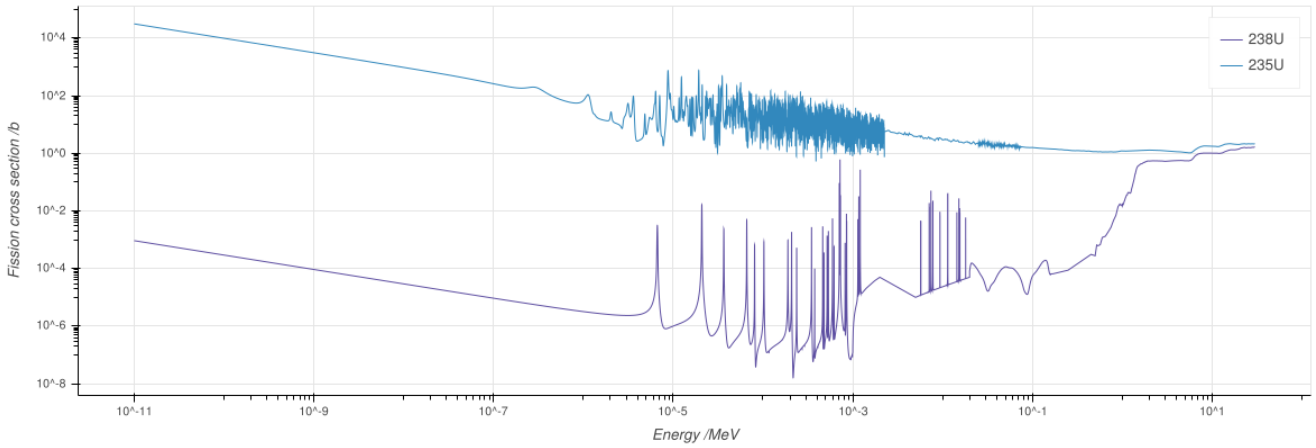

Figure 6: Fission cross sections of ^{238}U and ^{235}U

average number of collisions required to thermalise a fast neutron increases by a factor $\frac{\xi_{H_2O}}{\xi_C} = 5.8$. However, the scattering to capture ratio of graphite is far higher than that of light water (1500 vs 77.17), and thus its effective "moderating ratio" $\frac{\xi\sigma_s}{\sigma_a}$ is greater. This result was observed in the predicted k_{eff} for the two systems. In the case of the graphite moderator, k_{eff} was greater (closer to criticality) than that of the light water. For both moderators, the application of the Shapiro–Wilke (W) test for normality indicated that the results are normally distributed with a 95 % confidence interval for all of the reactivity estimators.

4.2.2 Increasing Enrichment

After increasing the enrichment of the uranium cylinders, the k_{eff} of both modelled systems was observed to increase. Similarly to the previous configuration, the predicted coefficient for the graphite moderator remained greater than that of the light water. As for the previous scenario, the application of the Shapiro–Wilke (W) test for normality indicated that the results are normally distributed with a 95 % confidence interval for all of the reactivity estimators.
The observed increase in reactivity derives from the increased effective fission cross section of the fuel that follows fuel enrichment (see Fig 6). ^{235}U has a greater fission cross section than ^{238}U, and thus increasing the ratio of ^{235}U to ^{238}U in the fuel serves to increase the fission probability, moving the system towards criticality.

5 Conclusions

In completing the two exercises, several important observations were made concerning the various MCNP features which may be used to ensure valid results, and identify problematic cases (such as undersampled paths). The final exercise shows explicitly the importance of selecting the correct fuel enrichment, and moderator material, to avoid a reactor becoming supercritical on prompt neutrons alone.

References

[1] Wunna Ko. *The Attenuation of Neutrons in Barite Concrete*.

[2] *Nuclear Reactor Types*. English. 2017, pp. 103–116.